DEFORMATION FIELDS ESTIMATION USING FIBER BRAGG GRATINGS

Stephan Rapp

Institute of Lightweight Structures, TU Muenchen,

Boltzmannstr. 15 85747 Garching

A possible approach to meet the increasing performance requirements of aerospace structures is the design of smart structures, which may provide different integrated functions. In applications like large, high precision and space reflectors or high aspect ratio airplane wings, were aeroelastic effects play a big role, the structures shape itself is of interest. The knowledge of static and dynamic deformations of these structures would provide the possibility to increase their performance by appropriate countermeasures. During operation, however, the monitoring of deformations of such large areas is often difficult. A solution is the here presented estimation of deformation fields using in plane strain data. The use of fibre Bragg grating (FBG) strain sensors for this application offers an integrated sensor network including a lot of measurement points within only a few channels. Besides deformations, temperatures could be another point of interest. For example temperature fields on airplane wings during supersonic flight. This kind of problem could be handled using similar methods and sensor networks. This paper discusses the deformation field estimation of a dynamically excited plate using a transformation matrix based on a modal approach. To reduce systematic estimation errors due to aliasing, a parameter study was performed and the sensor locations were optimized. In an experiment a cantilever plate was equipped with 16 FBG sensors in an optimized configuration to verify the estimation and optimization methods.

1. INTRODUCTION

The performance requirements of modern aerospace structures are increasing continuingly. Thereby the condition monitoring of structures plays a key role. One of the items of interest is the shape of the structure itself. Examples can be large, high precision and space reflectors or airplane wings and control surfaces. Especially high aspect ratio wings, were aeroelastic effects play a big role, might be a possible application for the monitoring of deformations. Or think about the future of morphing structures, where large, global deformations will occur and have to be controlled. But in a lot of applications the direct measurement of dynamic deformations of large areas is very difficult, especially during operation. Thus one has to think about alternatives of monitoring shapes of extended structures. Possible properties which could be measured and related to deformations can be, amongst others, accelerations or strains. Both physical values have their advantages. Accelerations are very sensitive signals in dynamic applications and they offer direct information about loads, furthermore they offer the possibility of monitoring rigid body motions. Their drawback is the disability of measuring static deformations. Strains on the other hand offer the possibility of measuring dynamic deformation effects as well as static ones, but rigid body motions can’t be recorded. However it seems to be easier to record the rigid body motions (6 degrees of freedom) with an additional sensing system than monitoring the static deformation field separately. Thus the usage of strains for this application seems to be advantageous. A look on the sensor level will approve this suggestion. If we assume, that the equipped structures are basically lightweight structures and a lot of measurement points are necessary we should think about a lightweight sensor and harnessing too. Thus both, accelerometers and origin strain gages show disadvantages. If going one step further and think about the integration of sensors into composite or even in membrane structures, these sensors have a lot of disadvantages. But there is a sensor type, the fibre optic sensor (FOS), which satisfies all these requirements. The FOS is lightweight itself, offers the possibility to multiplex up to 60 sensors within one fibre and is, due to its small dimensions (diameter < 250µm), feasible to integrate into composites. The FOS can be used as a strain sensor as well as a temperature sensor. Since the monitoring of temperature fields on large aerospace structures might be of interest too, think of the thermal loads on airplane wings during supersonic flight, the use of FOS for the monitoring network is very interesting.

With this background the use of strain data as a basis for deformation monitoring seems to be defensible. But beside this elementary question about the measured physical value a lot of other questions have to be answered if the desired monitoring task ought to be handled satisfactory. An obvious question is the one about the estimation approach. How to relate strains to deformations? Furthermore the sensor amount and their locations have to be designated. Beside these questions about the estimation technique it might be interesting how the loading conditions influence the estimation quality.

In the following these questions, which are a choice amongst others, will be discussed. Before the theoretical background for these questions will be given, the fibre Bragg grating sensor will be introduced.

2. THEORETICAL BACKGROUND

2.1. Fibre Bragg Gratings

As mentioned in the introduction the use of fibre optic sensors (FOS) for distributed strain sensing offers a lot of advantages. Especially the fibre Bragg grating (FBG) sensor, which is one type of FOS, fits very well to this kind of application. The working principle of the FBG is based on a periodic change of the refractive index in the optical fibre, such that a special wavelength, the Bragg wavelength λ_B, is reflected at this grating. The Bragg wavelength is defined as,

$$(1) \quad \lambda_B = 2 \cdot \Lambda \cdot n_0$$

where Λ is the period of imperfections and n_0 the refractive index of the core. Using a high intensity UV-laser, the grating can be written into the optical fibre using a template called phase mask. If different phase masks are used, gratings with different Bragg wavelength λ_B can be written. Thus it is possible to write different unique gratings into one fibre. This enables the multiplexing of a lot of sensors within a single fibre. Using the different wavelengths it is possible to relate the reflected sensor signal to a designated location. This wavelength-division multiplexing technique offers the possibility of extensive sensor networks on large areas using only a few sensor fibres.

If strain, mechanical or thermal, is applied to the fibre the gratings differ from each other and the reflected wavelength is changed (see FIG 1).

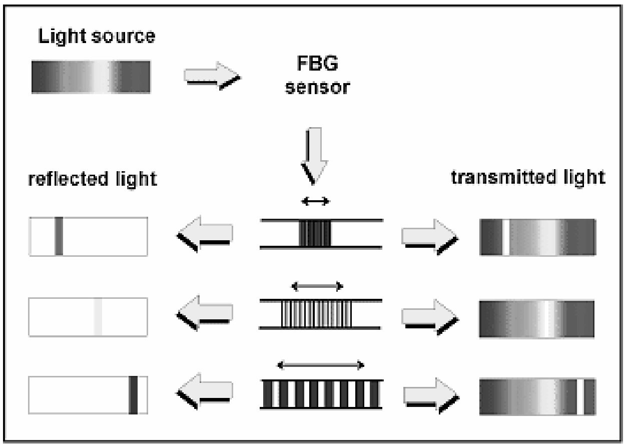

FIG. 1 FBG strain sensor working principle

The wavelength shift can be derived using the following equation.

$$(2) \quad \frac{\Delta\lambda}{\lambda_B} = (1 - p_{eff}) \cdot \Delta\varepsilon + [(1 - p_{eff}) \cdot \alpha_T + \frac{1}{n_0}\frac{dn}{dT}] \cdot \Delta T$$

Thereby $\Delta\lambda$ is the wavelength shift, p_{eff} the photo-elastic coefficient, $\Delta\varepsilon$ the change of mechanical strain, α_T the coefficient of thermal expansion, $\frac{dn}{dT}$ the photo-thermal coefficient and ΔT the change of temperature. Since in laboratory conditions the temperature changes marginally and the performed experiments were within only a few minutes of duration the effect of changing temperatures could be neglected. Thus equation (2) simplifies to

$$(3) \quad \frac{\Delta\lambda}{\lambda_B} = (1 - p_{eff}) \cdot \Delta\varepsilon$$

2.2. Deformation Fields Estimation

In the subsection before we saw that the use of FBG sensors offers a lot of advantages if they are used for a (integrated) sensor network in lightweight structures. The output of this sensor network is mechanical or thermal strain at discrete locations. To get information about the required deformation field of a structure, one has to estimate the field using discrete strain data. This is a challenging task, since there are two problems to deal with. The one is the interpolation of a field and the other is the relating of deformations and strains. The task becomes even more complex if the field has to be estimated dynamically and without any time delay. If that isn't required, the use of calibration[1] or transfer functions[2] is possible. Thereby strains and deformations are measured and related to each other before the field is estimated afterwards.

For the dynamic deformation fields estimation another approach is followed here. As we know it is possible to approximate a dynamic deformation field using shape functions, called mode shapes and corresponding weighting factors, called modal coordinates q. Since in most technical applications only the first few mode shapes are of interest, think of the first bending of an airplane wing, its first torsion mode and the combination leading to flutter. In these first modes the amplitudes are high and a lot of structural mass is involved, what leads to high loads. The deformation effects of higher modes can be neglected. This effect is used for the modal reduction. That means that only a few mode shapes are used to approximate the structures behaviour. The same approach can be used to express dynamic strain fields. The linear combination of mode shapes can be expressed in a matrix notation showed in equations (4) and (5).

$$(4) \quad \{w\}_{Nx1} = [\Phi]_{Nxn} \cdot \{q\}_{nx1}$$

$$(5) \quad \{\varepsilon\}_{Mx1} = [\Psi]_{Mxn} \cdot \{q\}_{nx1}$$

Thereby {w} is the displacement vector, N is the number of discrete displacements, $[\Phi]$ is the matrix of deformation mode shapes, n is the number of used mode shapes to approximate the real deformation, {q} is the vector including the corresponding weighting factors, called modal coordinates. $\{\varepsilon\}$ is the vector of M discrete strain values, $[\Psi]$ is a matrix including the strain mode shapes.

As one can see, the modal coordinates q, are the same for the deformation and strain equation. Using some mathematical calculations it is possible to relate the deformations to the strains.

$$(6) \quad \{w\}_{Nx1} = \underbrace{[\Phi] \cdot ([\Psi]^T \cdot [\Psi])^{-1} \cdot [\Psi]^T}_{[SDT]_{NxM}} \cdot \{\varepsilon\}_{Mx1}$$

The Strain-Deformation-Transformation Matrix (SDT) connects a vector of M strain values with a vector of N deformation values, thus it is possible to estimate a deformation field using only a few discrete strains. Since in equation (6) it is assumed that the strain field consists of a finite number of mode shapes n, the estimated deformation vector $\{\hat{w}\}$ will differ from {w}, if real strains $\{\bar{\varepsilon}\}$ consisting of an infinite number of mode shapes is used in the deformation estimation process.

(7) $\{\hat{w}\} = [SDT]\{\bar{\varepsilon}\} \neq \{w\}$

This circumstance induces a systematic estimation error, which can be explained as aliasing. Shares of the strain signal of higher order frequencies might be interpreted wrongly. This effect is much the worse, since higher order strain mode shapes can't be neglected as it is the case for higher order displacement mode shapes. Since the frequency goes down to the strain shapes amplitude with squares, the higher order strain mode shapes have still high shares.
To minimize this effect the number of sensors and especially their location has to be adequate. But if one assumes an unknown excitation, the decision for sensor locations is difficult. In this case it would be advantageous to find a general parameter, depending on the sensor locations, which promises good estimation results.

2.3. Condition Number (CN)

One such general parameter might be the condition number (CN) of the transformation matrix as Chen-Jung Li et. al.[3] showed. The condition number of a matrix indicates its conditioning. It is an indicator for the information conservation during matrix operations. The smaller the condition number, the better the conditioning of the matrix. The minimum value of the CN is 1. The mathematical definition of the condition number is the ratio of the largest to the smallest singular value of a matrix. It can be calculated by the product of the matrix norm and the norm of the inverse (eq. 8 and eq. 9).

(8) $CN = \left\|[SDT]\right\| \cdot \left\|[SDT]^{-1}\right\|$

(9) $\left\|[SDT]\right\| = \sqrt{tr([SDT]\cdot[SDT]^T}$

Thereby $\left\|[SDT]\right\|$ is the matrix norm and tr is the trace of the matrix. Equation (9) indicates one definition of the matrix norm. Since the SDT, thus the CN, is depending on the sensor locations and, as we will see, is an indicator for good estimation quality, it was used as the objective function for the sensor placement optimization. Thereby an optimization algorithm provided by Matlab used the implemented function '*cond*' to calculate the condition number.

2.4. Coordinate Transformation

Since in this study a two dimensional plate was investigated and the in plane movement was assumed to be much smaller than the out of plane deformations, the deformation field consisted of a scalar value, the out of plane deformation, at each discrete point. Thus the deformation field can be described using a vector (see eq. 4). For the strain it is different. Even in a two dimensional case there are three components of strain at one point, normal strain in x and y direction and shear. If the introduced approach with the strain-deformation matrix SDT shall be used, we have to use a strain mode shape matrix $[\Psi]$ with a single degree of freedom at every location. For that a coordinate transformation equation (10)[4] was used, which transforms strain from the x- and y-direction and shear into strain in an arbitrary direction x' (see FIG. 2).

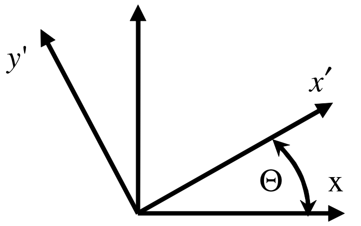

FIG. 2 Coordinate transformation

To perform the transformation the following equation was used.

$$\varepsilon'(t) = \frac{\varepsilon_x(t)+\varepsilon_y(t)}{2} + \frac{\varepsilon_x(t)-\varepsilon_y(t)}{2}\cos 2\Theta + \frac{1}{2}\varepsilon_{xy}(t)\sin 2\Theta \quad (10)$$

The same transformation approach was applied to the mode shape matrices of the different components.

$$[\Psi] = \frac{[\Psi_x]+[\Psi_y]}{2} + \frac{[\Psi_x]-[\Psi_y]}{2}\cos 2\Theta + \frac{1}{2}[\Psi_{xy}]\sin 2\Theta \quad (11)$$

Thus the calculated matrix $[\Psi]$ could be used in equation (6).

3. SIMULATION

Using different simulation tools, parameters like the condition number, the number of sensors and the excitation frequency were investigated. Therefore the following simulation model was used.

3.1. Simulation model and process

A cantilever plate with the dimensions of 900 x 600 mm and a thickness of 8 mm (see FIG. 3) was discretized with 30 x 20 shell elements in a FEM model.

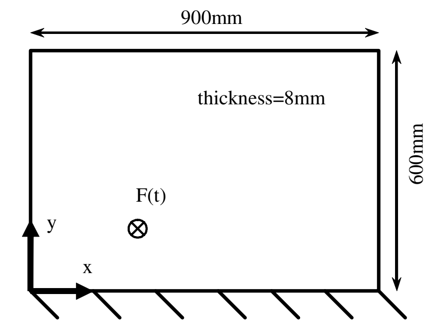

FIG. 3 Simulation model

The excitation (F(t)) location was defined with respect to the experimental set up to x = 330 mm and y = 180 mm. The location in x direction was chosen to avoid the application of forces in a nodal line of the first three eigenmodes, which can be seen in FIG. 4. The corresponding natural frequencies are $\omega_1 = 6{,}83Hz$, $\omega_2 = 12{,}48Hz$ and $\omega_3 = 28{,}18Hz$.

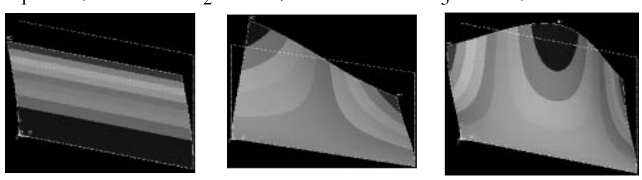

FIG. 4 Displacement mode shapes

The first step in the simulation was the determination of the displacement and strain mode shapes using a FEM model. After that, these mode shapes were exported to a matlab script, which was used to perform a state space simulation of the excited plate. The output of this simulation were the approximated time depending, real deformation and strain fields according to the applied excitation. Beside that the mode shapes were used in combination with the used measurement locations to determine the SDT. Using the approximated strain data at the assumed measurement points and the SDT the deformation field could be estimated. At the end the estimated field could be compared with the approximated real field and evaluated by calculating the RMS[5].
The flow chart in figure 5 shall illustrate the simulation process.

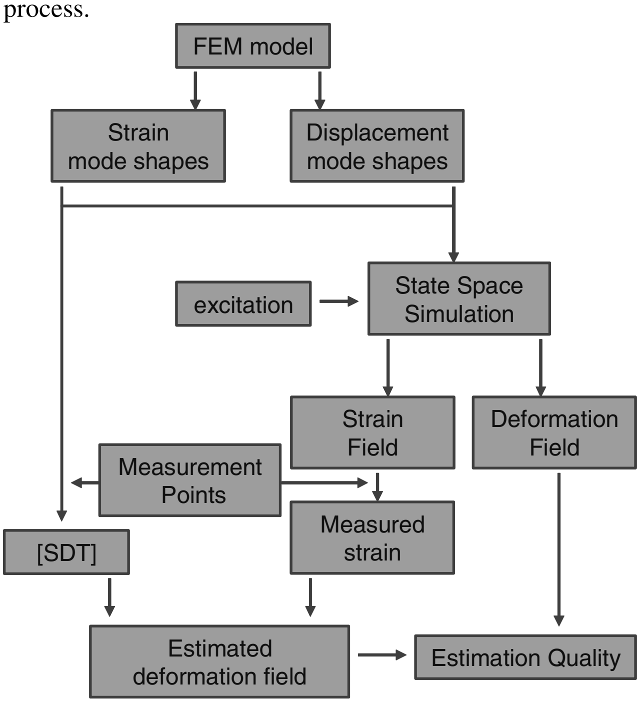

FIG. 5 Simulation flow chart

3.2. Parameter study

In the introduction it was mentioned, that a lot of parameters have to be considered and investigated to accomplish the aspired deformation field estimation task. Here the results of the investigations of a sample of parameters are presented. These parameters are:

- Condition number (CN)
- Sensor amount
- Excitation frequency

As mentioned before, in the literature it can be found that, the condition number of a transformation matrix is an indicator for good estimation results[3]. Furthermore in general the condition number is used to evaluate mapping functions. To verify the use of the condition number as a general indicator, the estimation results of several configurations were correlated to the corresponding condition numbers. Therefore ten sensor configurations, with eight randomly distributed sensors each, were used in the simulation and the resulting estimation error was plotted against the condition number. Thereby the excitation was a sinusoidal signal with a frequency of 10Hz. The correlation between the estimation results and the condition numbers are summarized in FIG. 6.

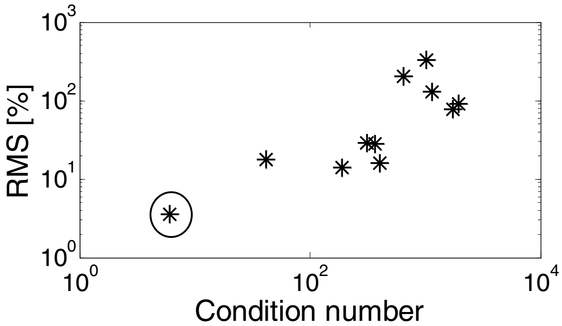

FIG. 6 RMS regarding the condition number

As one can see, the dispersion of the values is quite high. This can be explained with the influence of two effects. The optimum of the condition number regarding the estimation error is very smooth[3], such that changes within the same magnitude hardly change the estimation results. That's why other effects, like the strain level at the measurement points, play bigger roles. To improve the optimization process another objective function, including the condition number and the strain level might be used. This parameter, called effectiveness, was investigated by Uwe Stöbener et. al[6]. The other reason might be the highly convex function of the condition number. Since a gradient searching algorithm was used to find the optimum, the starting value was a decisive parameter. That's why there couldn't be a guarantee to find the absolute optimum, despite a lot of starting values were used. The use of genetic algorithms might improve the optimization process. Nevertheless, the trend is obvious, if the condition number changes with magnitudes, the estimation error changes with magnitudes too.
Beside the ten random distributions the value for the condition number minimized sensor distribution is showed, marked with a circle. One can see that the estimation quality is much better than that of the other configurations, thus the use of the condition number as a general indicator for high estimation quality was verified. With the use of condition number minimized sensor locations, the question about the sensor alignment is dispensable. Although the sensor location itself shows the higher effect on the estimation quality[5] it is not a general approach. Depending on the structure and especially the load case, one would locate them at other positions. Thus a general conclusion about the sensor location is very difficult.
Another parameter, which influences the estimation quality significantly, is the sensor amount. The presumption that an increasing number of sensors would increase the estimation quality was investigated and the results are presented here. For the investigation, condition number minimized sensor distributions were chosen. The relationship between the number of sensors and the estimation error, evaluated using the RMS, is illustrated with the diagram in figure 9. The results reference a sinusoidal excitation with a frequency of 10 Hz. The presumed improvement of the estimation with an increasing number of sensors was confirmed with these results.

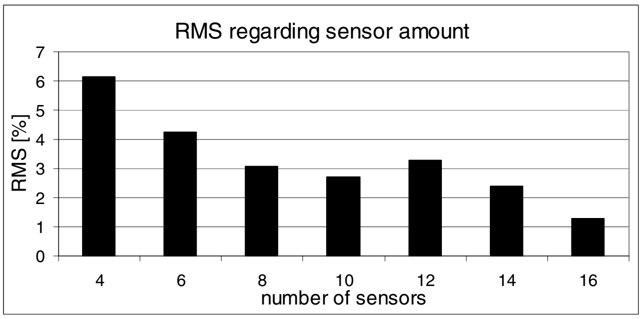

FIG. 7 Estimation error regarding sensor amount

The investigations of the condition number and the sensor amount were performed using an excitation frequency of 10 Hz. This note is important, since the estimation result depends strongly on the loading conditions. One can distinguish two different kinds of dynamic loads, harmonic and random excitations. Here the influence of different harmonic, sinusoidal signals was investigated. Using 16 sensors in a condition number optimized configuration the system was simulated using six different excitation frequencies. The resulting estimation errors are summarized in figure 8.

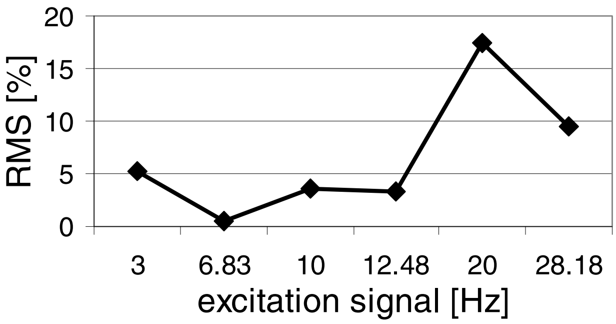

FIG. 8 Estimation error regarding excitation frequency

The curve shows two characteristic properties.

- Increasing estimation error with increasing excitation frequency even for resonance excitations
- Higher estimation errors for off resonance excitations compared to the errors for resonance excitations

The first effect might be explained with the influence of residual modes. The higher the excitation frequency, the nearer the residual modes are, thus their influence might increase. A possible explanation of the second property is the more complex deformation of the plate including shares of different mode shapes if it is excited with a frequency between two eigenfrequencies.

At the end of this section a figure shall illustrate the deformation estimation and give an idea of the quantitative value of the RMS. Figure 9 shows a real and estimated deformation field for a 10 Hz excitation, determined using 16 sensors in an optimized distribution. With an estimation error of RMS = 3.54%, the two surfaces cover each other quite well.

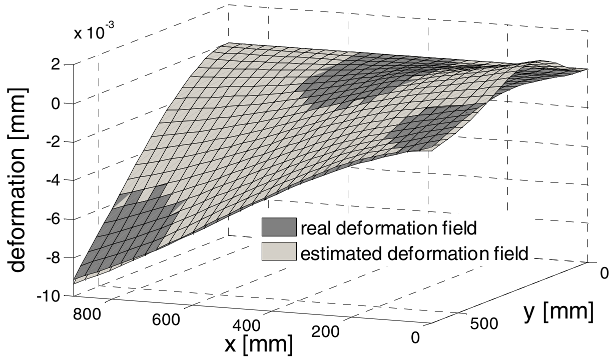

FIG. 9 Deformation Field: 10 Hz, RMS = 3.54%

4. EXPERIMENT

4.1. Set up

The performed parameter studies presented in the section before showed, that a certain amount of sensors is necessary, with respect to the expected excitation, to achieve a satisfactory estimation quality. Furthermore the determination of the sensor distribution using the condition number of the transformation matrix as an objective function in an optimization algorithm proofed to be successful. Thus an experimental plate was equipped with 16 fibre Bragg grating strain sensors in a condition number minimized configuration. The number of sensors was limited to 16 due to the experimental device. To reduce the optimization variables from 48 to 16, the orientations of the sensors were fixed into x and y direction at each location, thus only x and y coordinates for 8 locations had to be determined. The optimized sensor locations, marked with a +, can be seen in the figure below.

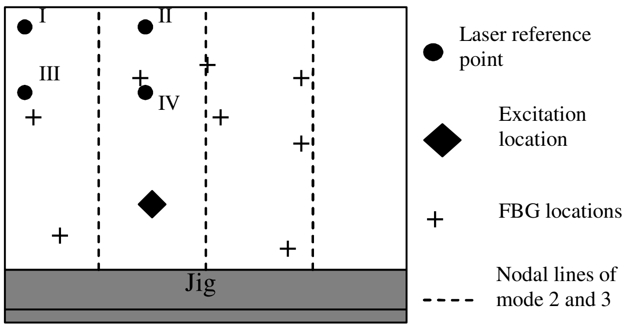

FIG. 10 Sensor set up

Beside the 8 sensor crosses including two rectangular strain sensors each, the excitation location and the locations of the reference sensors I, II, III and IV can be seen. These locations were determined regarding the following criteria.

- Avoiding the location at nodal lines
- Asymmetric alignment to increase the amount of information
- Separated distribution to increase the amount of information
- Placed at locations with high deflections to remain in the resolution range of the reference sensing system

The used reference measurement system consisted of four laser sensors, their controller units and a computer for the data processing. The excitation was applied by a modal shaker. The shaker was connected to the plate by a slight rod. This rod was used to avoid transversal forces or even moments, thus only out of plane forces were applied to the plate. A function generator provided the sinusoidal signal. The signal was amplified and forwarded to the shaker. The attitude of the four reference sensors and the modal shaker with respect to the cantilever plate can be seen in figure 11.

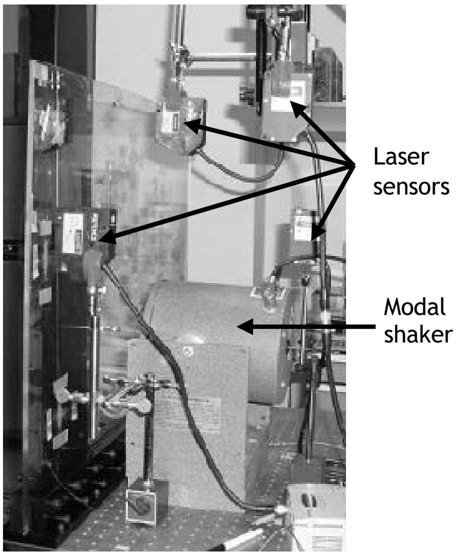

FIG. 11 Reference sensors and shaker

The cantilever plate, consisting of acrylic, was mounted on the experimental table using a steel jig. To enable the measurement of strain in x and y direction at the same location, 8 FBG strain sensors were mounted at the top side of the plate and 8 sensors at the same location at the bottom side. Thereby 4 sensors were multiplexed within one fibre by using the wavelength division multiplexing technique. That means that every sensor in one sensor fibre has had a unique Bragg wavelength. Thus 4 measurement channels were used to collect the strain data of 16 measurement points. The equipped plate with the 8 FBG crosses, marked with circles, can be seen in figure 12.

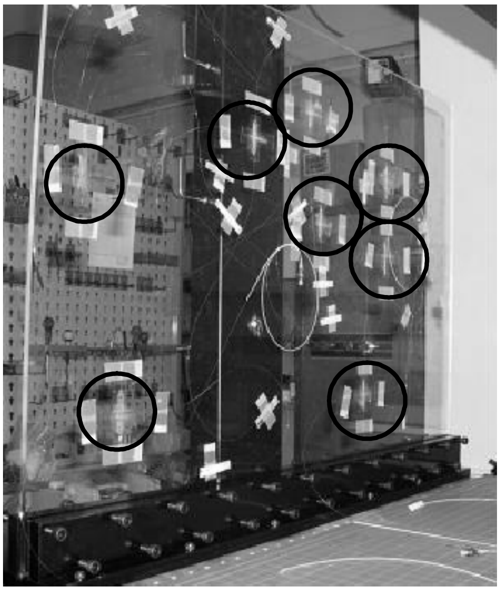

FIG. 12 Equipped plate

The fibre optic interrogation unit consisted of the sensor fibres, a broadband light source, the spectrometer and the data processing computer. The spectrometer worked using a fibre Fabry-Perot filter.

4.2. Experimental Results

Using the measured strains, the deformation field could be estimated. Comparing the deformation values of the reference measurement system to the estimated deformations at the corresponding locations, the estimation error (RMS) could be calculated. Since the deformation and strain data couldn't be collected time synchronously, the time axis of deformation and strain measurements were adjusted. Thereby the time axis of the deformations was moved until the deformation response of one reference point covered one characteristic strain curve. Thus no phase shift effects could be considered in the error calculation. The determined estimation errors are summarized in table 1.

TAB. 1 Experimental results

Excitation frequency [Hz]	RMS [%]
3	0.56
7.14	0.44
10	1.31
12.84	0.46
20	1.12
31.08	2.20

One can see that the RMS values are very small. That shows the potential of this kind of estimation approach. However one has to say, that only four points were used to calculate the estimation error, furthermore the phase shift effects were excluded. Nevertheless the estimation quality was satisfactory. This can be illustrated with figure 13 and 14. Figure 13 shows the time response at reference point I for a 10 Hz excitation. Thereby the dashed line represents the measured deformation signal and the full line the estimated deformation at this node. Figure 14 shows the estimated deformation field for a certain time step.

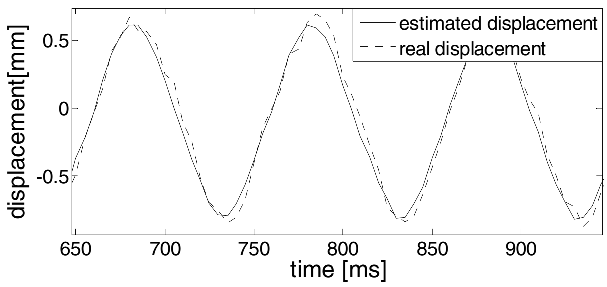

FIG. 13 Time response for 10 Hz excitaiton at point I

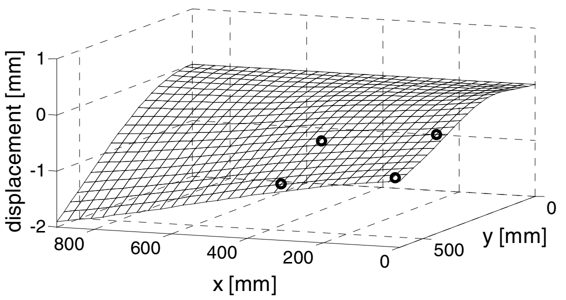

FIG. 14 Estimated shape for 10 Hz excitation

The figure includes the for measured reference points, which are covered well by the deformation field.

4.3. Correlation

Despite the quantitative values for the estimation errors of the simulation and the experiment can't be compared since in the experiment only four points were considered in the error calculation and the phase shift effects were excluded, it can be said that there is a quite good qualitative correlation. In table 1 it can be seen, that the errors in off resonance cases is much higher than in resonance cases. An exception is the result for the third resonance frequency excitation. This extraordinary high error can be explained with the limited sampling frequency of the interrogation unit, which used a buffer for the data transfer to the computer. Thus the measured strain signals for this frequency were very rough what resulted in unrepresentative estimation results for higher frequencies.

5. CONCLUSION

The simulation showed that the estimation approach using the mode shapes as shape functions works very well. If enough mode shapes, or sensors, respectively, were used, the estimation results were satisfactory. Especially if the global deformation of the structure is of interest, for example the global deflection of an airplane wing, this approach seems to be very good. If local effects, like the discrete load application with the modal shaker, play a role, the method shows disadvantages, since the shape functions can't map local effects.
The approach, using the condition number as the objective function for the sensor alignment optimization, was successful too. This approach is a very general one and has probably to be improved by some requirements or additional objectives to include structure dependent properties.
In the simulation it was figured out that the loading condition has a big influence on the estimation results. Although, unfortunately phase shift effects couldn't be considered in the experiment, the experimental results verified the simulation and showed especially the strong dependence of excitation and estimation quality.

6. OUTLOOK

To improve the estimation method different approaches can be followed. At first static deformation solutions can be included in the shape function basis to include the possibility of mapping local effects. Furthermore the optimization can be improved by using another objective function like the effectiveness introduced by Uwe Stöbener[6], or by inserting restrictions, for example minimum strain values. Using genetic algorithms would increase the probability of finding the global minimum.
To make the deformation estimation even more general it will be necessary to include additional sensors, for example accelerometers, to enable the detection of rigid body motions.

ACKNOLEDGEMENT

The author wants to acknowledge the support at KAIST (Korea advanced institute for science and technology) in Daejeon, South Korea, where the simulation and experimental work was done.

7. REFERENECES

[1] Peter Giesecke, „Dehnungsmessstreifentechnik – Grundlagen und Anwendungen in der industirellen Messtechnik“, Vieweg, Wiesbaden, Germany, 1994

[2] Attilio C. Pisoni, Claudio Santolini, Dagmar E. Hauf, Steven Dubowsky, "Displacements in a vibrating body by strain gauge measurements", Proceedings of the 13th Internatinal Conference on Modal Analysis, 1995

[3] Chen-Jung Li, A. Galip Ulsoy, "High-Precision Measurement of Tool-Tip Displacement Using Strain Gauges in Precision Flexible Line Boring", Mechanical Systems and Signal Processing, 13, p. 531-546, 1999

[4] Andrew Pytel, Jaan Kinsalaas, "Mechanics of materials", Thomson Brooks/Cole, Pacific Grove, 2003

[5] S. Rapp, L.H. Kang, U.C. Mueller, J-H. Han, H. Baier "Dynmaic shape estimation by modal approach using fiber Bragg grating strain sensors", Smart Structures and Materials 2007 - Sensors and Smart Structures Technologies, 18. - 22. März 2007, San Diego, CA, USA Proceedings of SPIE Vol. 6529

[6] Uwe Stöbener, Lothar Gaul, "Modal Vibration Control for PVDF Coated Plates", Journal of Intelligent Material Systems and Structures, 11, p. 283-293, 2000